

# Primordial non-Gaussianity with CMB spectral distortions: trispectrum and scale dependence

Michele Liguori

Dipartimento di Fisica e Astronomia G. Galilei

Università di Padova

Work in collaboration with N. Bartolo, A. Ravenni, M. Shiraishi

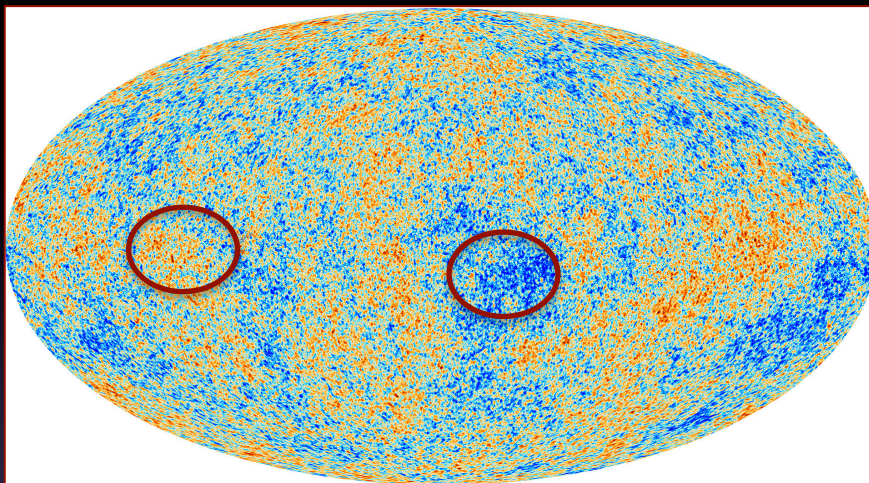
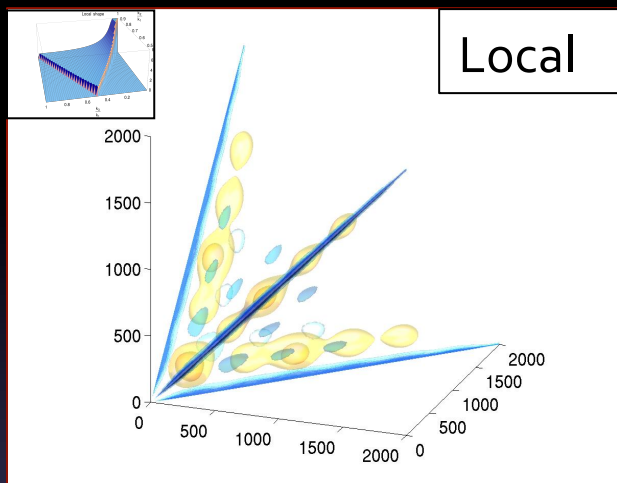
Based on:

N. Bartolo, ML, M. Shiraishi (2015) arXiv: 1511.01474

A. Ravenni, ML, N. Bartolo, M. Shiraishi (2017) arXiv: 1707.04759

# Squeezed bispectrum and spectral distortions

Squeezed bispectra generate couplings between large and small scales i.e., large scale modulation of small scale power



This modulation couples CMB temperature fluctuations on large scales to spectral distortions arising from acoustic wave dissipation at very small scales.

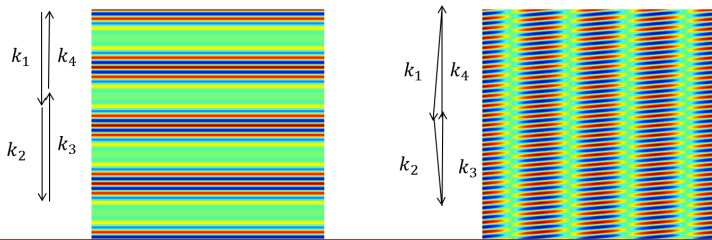
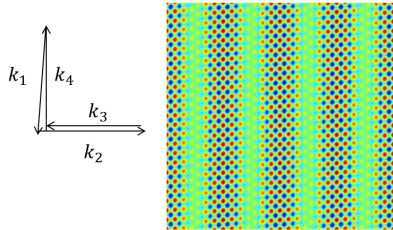
- Use  $T_{\mu}$  to measure local  $f_{\text{NL}}$  (Pajer and Zaldarriaga 2013)
- Further constraining power on  $f_{\text{NL}}$  running (Biagetti et al. 2013, Emami et al. 2015)
- Large S/N increase for “super-squeezed” shapes (Ganc and Komatsu 2013)

What can we say about trispectra?

# Trispectrum

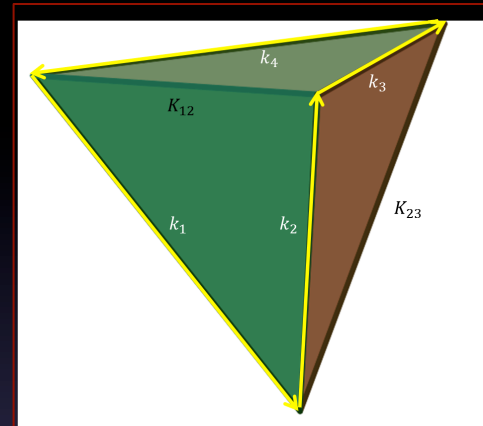
$$\langle \Phi(k_1)\Phi(k_2)\Phi(k_3)\Phi(k_4) \rangle \propto F(k_1, k_2, k_3, k_4, K_{12}, K_{23}) \delta(\vec{k}_1 + \vec{k}_2 + \vec{k}_3 + \vec{k}_4)$$

Diagonal squeezed trispectra  $|k_1| \sim |k_2|, |k_3| \sim |k_4|, |k_1 + k_2| = |k_3 + k_4| \ll |k_2|, |k_3|$



Diagonal squeezed trispectrum:  $\tau_{NL}$

$$\tau_{NL} < 2800 \quad (95\% \text{ C.L.})$$

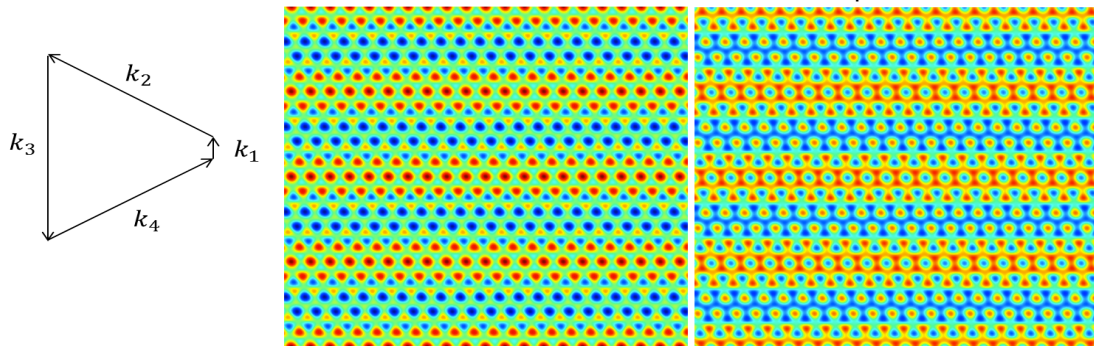


Pictures from Lewis(2012)

One-leg squeezed trispectra  $|k_1| \ll |k_2| \sim |k_3| \sim |k_4|$

Trispectrum > 0

Trispectrum < 0



Leg squeezed trispectrum:  $g_{NL}$

$$g_{NL}^{local} = (-9.0 \pm 7.7) \times 10^{-4}$$

# Trispectrum and spectral distortions

- The  $\mu\mu$  spectrum can be used to measure small scale modulation of power due to a squeezed diagonal trispectrum. Sensitivity to  $\tau_{\text{NL}}$  (flat  $\mu\mu$  spectrum in the Gaussian, stationary case)
- $T(T\mu)$  can measure large scale modulations of the bispectrum -> sensitivity also to  $g_{\text{NL}}$

$$\zeta(\mathbf{x}) = \zeta^{\text{G}}(\mathbf{x}) + \frac{9}{25}g_{\text{NL}} (\zeta^{\text{G}}(\mathbf{x}))^3$$

$$\zeta(\mathbf{x}) = \zeta_{\text{S}}(\mathbf{x}) + \zeta_{\text{L}}(\mathbf{x}) = \zeta_{\text{S}}^{\text{G}}(\mathbf{x}) + \zeta_{\text{L}}^{\text{G}}(\mathbf{x}) + \frac{27}{25}g_{\text{NL}}\zeta_{\text{S}}^{\text{G}}(\mathbf{x}) (\zeta_{\text{L}}^{\text{G}}(\mathbf{x}))^2$$

$$\zeta_{\text{S}}(\mathbf{x}) = \zeta_{\text{S}}^{\text{G}}(\mathbf{x}) \left[ 1 + \frac{27}{25}g_{\text{NL}} (\zeta_{\text{L}}^{\text{G}}(\mathbf{x}))^2 \right]$$

$$\frac{\delta\langle\zeta^2\rangle}{\langle\zeta^2\rangle} \simeq \frac{\delta\mu}{\mu} \simeq \frac{54}{25}g_{\text{NL}} (\zeta_{\text{L}}^{\text{G}}(\mathbf{x}))^2$$

$$\left\langle \frac{\delta T_1}{T} \frac{\delta T_2}{T} \frac{\delta\mu_3}{\mu} \right\rangle \simeq \frac{54}{25}g_{\text{NL}} \left\langle \frac{\zeta_1}{5} \frac{\zeta_2}{5} (\zeta_{\text{L}3}^{\text{G}})^2 \right\rangle = 108 g_{\text{NL}} \left\langle \frac{\delta T_1}{T} \frac{\delta T_3}{T} \right\rangle \left\langle \frac{\delta T_2}{T} \frac{\delta T_3}{T} \right\rangle$$

$$\langle\mu\rangle \simeq (9/4)A_S \ln(k_i/k_f) \Rightarrow b_{\ell_1\ell_2\ell_3}^{\text{TT}\mu} \simeq 108 g_{\text{NL}} \frac{9}{4}A_S \ln\left(\frac{k_i}{k_f}\right) C_{\ell_1}^{\text{TT}} C_{\ell_2}^{\text{TT}}$$

Same approach can be applied to  $\tau_{\text{NL}}$

$$\zeta(\mathbf{x}) = \zeta^{\text{G}}(\mathbf{x}) + \sqrt{\tau_{\text{NL}}}\sigma(\mathbf{x})\zeta^{\text{G}}(\mathbf{x})$$

$$\frac{\delta\langle\zeta^2\rangle}{\langle\zeta^2\rangle} \simeq \frac{\delta\mu}{\mu} \simeq 2\sqrt{\tau_{\text{NL}}}\sigma(\mathbf{x})$$

$$\left\langle \frac{\delta T_1}{T} \frac{\delta T_2}{T} \frac{\delta\mu_3}{\mu} \right\rangle \simeq 2 \left\langle \frac{\zeta_1^{\text{G}}}{5} \frac{\zeta_2^{\text{G}}}{5} [1 + \sqrt{\tau_{\text{NL}}}(\sigma_1 + \sigma_2)] \sqrt{\tau_{\text{NL}}}\sigma_3 \right\rangle$$

$$b_{\ell_1\ell_2\ell_3}^{TT\mu} \simeq 50 \tau_{\text{NL}} \frac{9}{4} A_S \ln\left(\frac{k_i}{k_f}\right) [C_{\ell_1}^{TT} + C_{\ell_2}^{TT}] C_{\ell_3}^{TT}$$

Full calculation is cumbersome. Formulae above reproduce quite accurately  
The exact behavior

# TTμ bispectrum, g<sub>NL</sub> contributions

$$b_{\ell_1 \ell_2 \ell_3}^{TT\mu} \simeq \frac{54}{25} g_{\text{NL}} \sum_{L_1 L_2} \frac{h_{L_1 L_2 \ell_3}^2}{2\ell_3 + 1} \int_0^\infty r^2 dr$$

$$\left[ \beta_{\ell_1}^T(r) \beta_{\ell_2}^T(r) \beta_{L_1}^\mu(r, z) \alpha_{L_2}^\mu(r, z) + \beta_{\ell_1}^T(r) \beta_{\ell_2}^T(r) \alpha_{L_1}^\mu(r, z) \beta_{L_2}^\mu(r, z) \right. \\ \left. + \beta_{\ell_1}^T(r) \alpha_{\ell_2}^T(r) \beta_{L_1}^\mu(r, z) \beta_{L_2}^\mu(r, z) + \alpha_{\ell_1}^T(r) \beta_{\ell_2}^T(r) \beta_{L_1}^\mu(r, z) \beta_{L_2}^\mu(r, z) \right]_f^i$$

$$\alpha_\ell^T(r) \equiv \frac{2}{\pi} \int_0^\infty k^2 dk \mathcal{T}_\ell(k) j_\ell(kr),$$

$$\alpha_\ell^\mu(r, z) \equiv \frac{3}{\pi} \int_0^\infty k^2 dk j_\ell(kx_{\text{ls}}) j_\ell(kr) e^{-k^2/k_D^2(z)},$$

$$\beta_\ell^T(r) \equiv \frac{2}{\pi} \int_0^\infty k^2 dk P(k) \mathcal{T}_\ell(k) j_\ell(kr),$$

$$\beta_\ell^\mu(r, z) \equiv \frac{3}{\pi} \int_0^\infty k^2 dk P(k) j_\ell(kx_{\text{ls}}) j_\ell(kr) e^{-k^2/k_D^2(z)}$$

In SW limit, using asymptotic approximations for integral of product of j<sub>l</sub> and for Wigner symbols, we recover previous result, modulo a pre-factor

$$b_{\ell_1 \ell_2 \ell_3}^{TT\mu, \text{SW}} \simeq \frac{972}{\pi} g_{\text{NL}} A_S \ln \left( \frac{k_i}{k_f} \right) C_{\ell_1, \text{SW}}^{TT} C_{\ell_2, \text{SW}}^{TT}$$

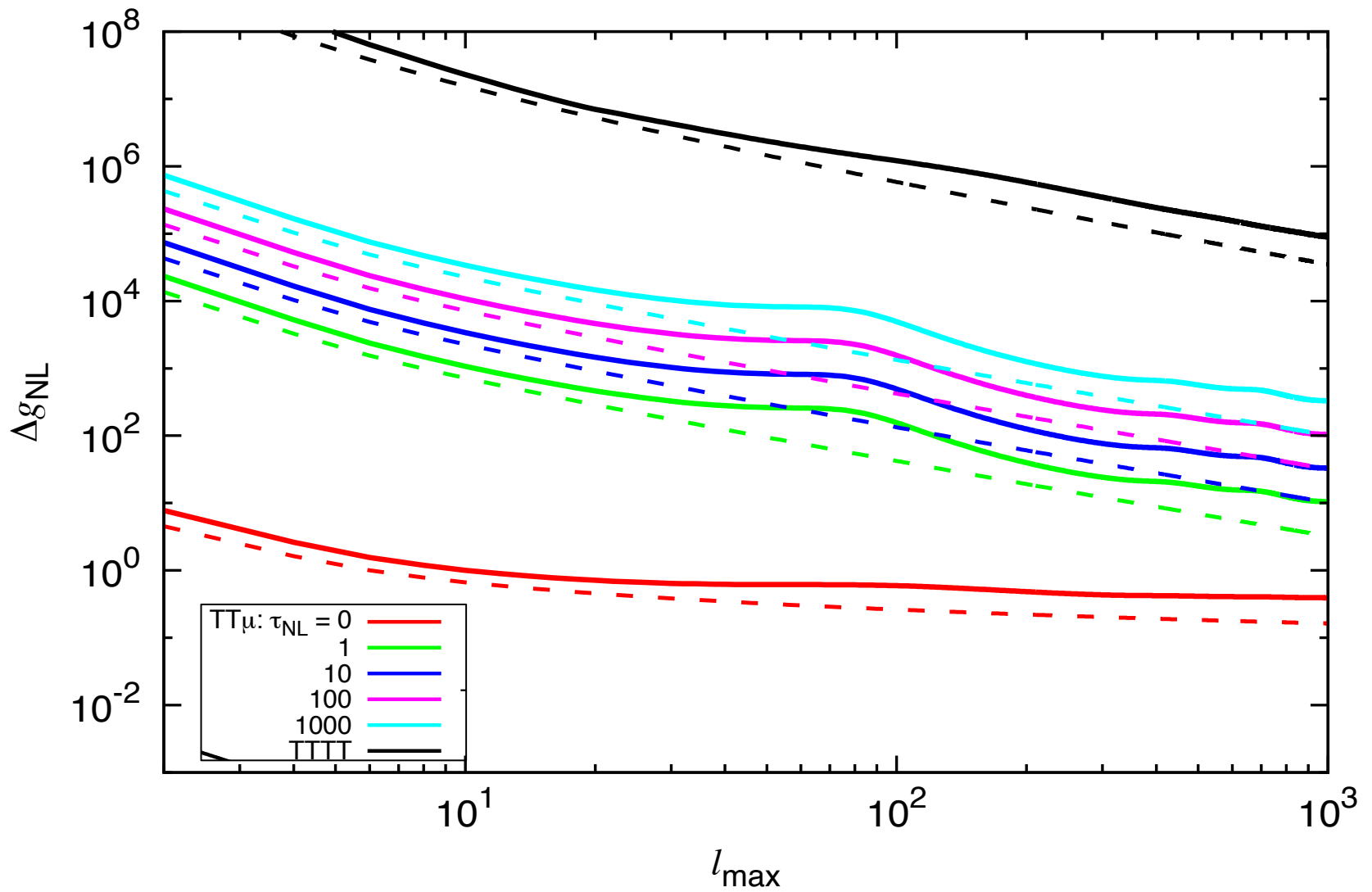
# Forecasts

Simple Fisher matrix forecasts (assuming perfect component separation)

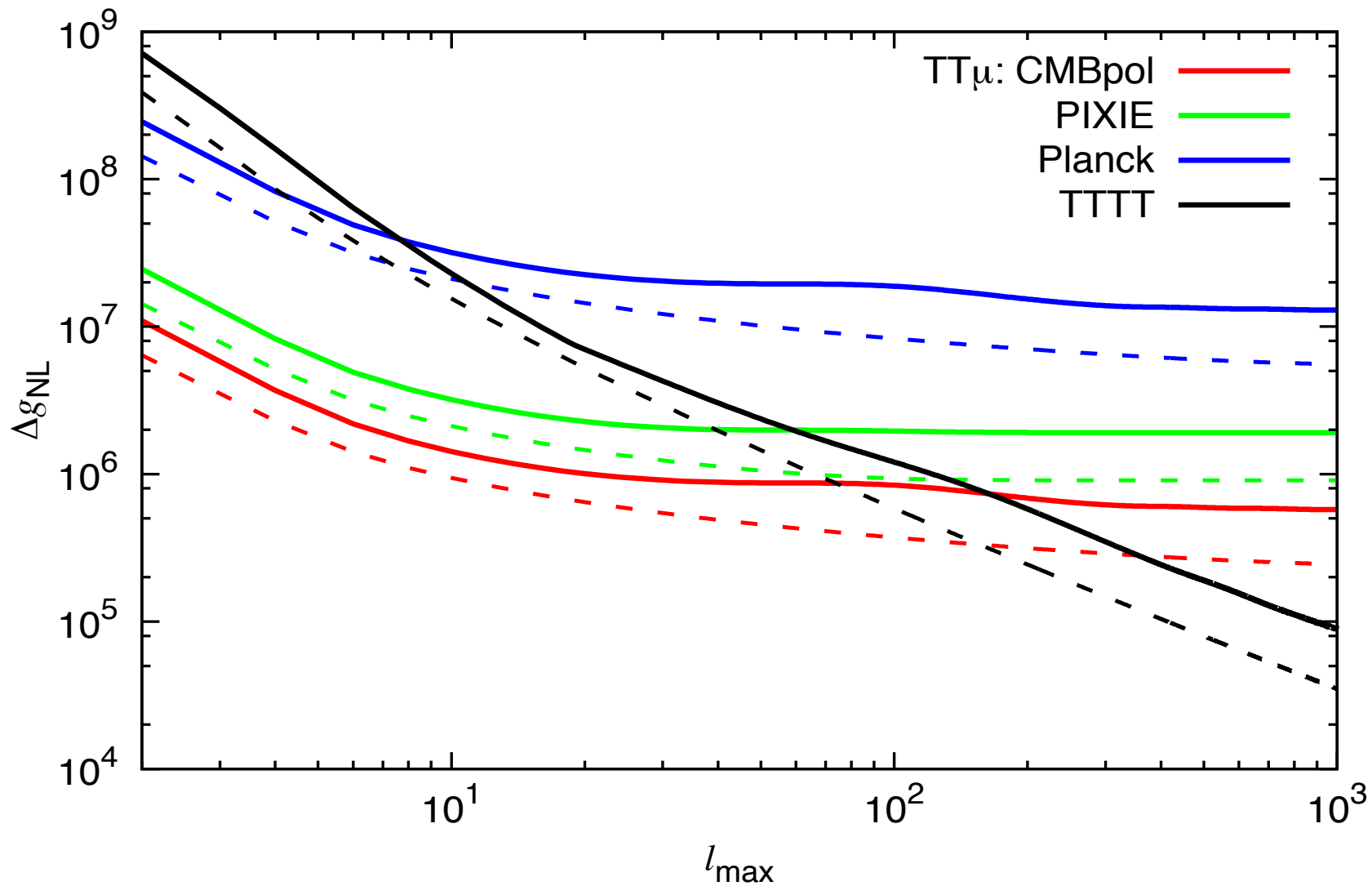
$$F^{TT\mu} = \sum_{\ell_1 \ell_2 \ell_3} \frac{\left( h_{\ell_1 \ell_2 \ell_3} \hat{b}_{\ell_1 \ell_2 \ell_3}^{TT\mu} \right)^2}{2C_{\ell_1}^{TT} C_{\ell_2}^{TT} C_{\ell_3}^{\mu\mu}}$$

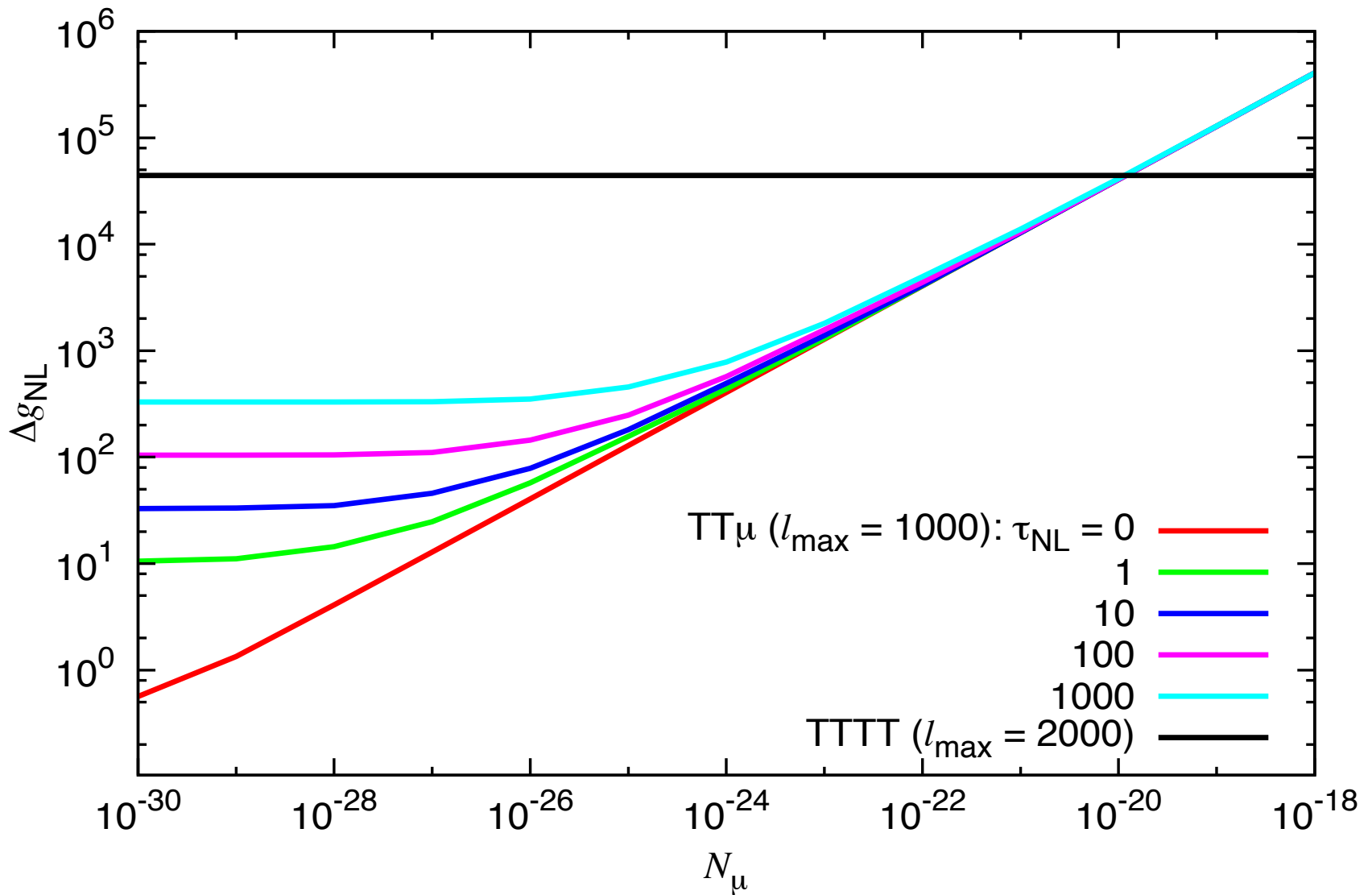
- Fiducial  $f_{\text{NL}} = 0$ . No  $T\mu$  terms in the variance
- $C^{\mu\mu}$  depends on  $\tau_{\text{NL}}$ .  $C^{\mu\mu, \tau_{\text{NL}}} \sim (5 \times 10^{-23} \tau_{\text{NL}} \text{ l}^{-2})$  dominates over Gaussian part,  $C^{\mu\mu, G} \sim 10^{-30}$ , if  $\tau_{\text{NL}}$  does not vanish
- We fix several values of  $\tau_{\text{NL}}$  and compute  $\Delta g_{\text{NL}}$  in each case
- S/N scaling, from flat sky approximation

$$\Delta g_{\text{NL}}|_{\tau_{\text{NL}}=0} \simeq \left( \frac{C_{\ell}^{\mu\mu, G}}{10^{-30}} \right)^{1/2} \left[ \ln \left( \frac{\ell_{\text{max}}}{2} \right) \right]^{-1}$$

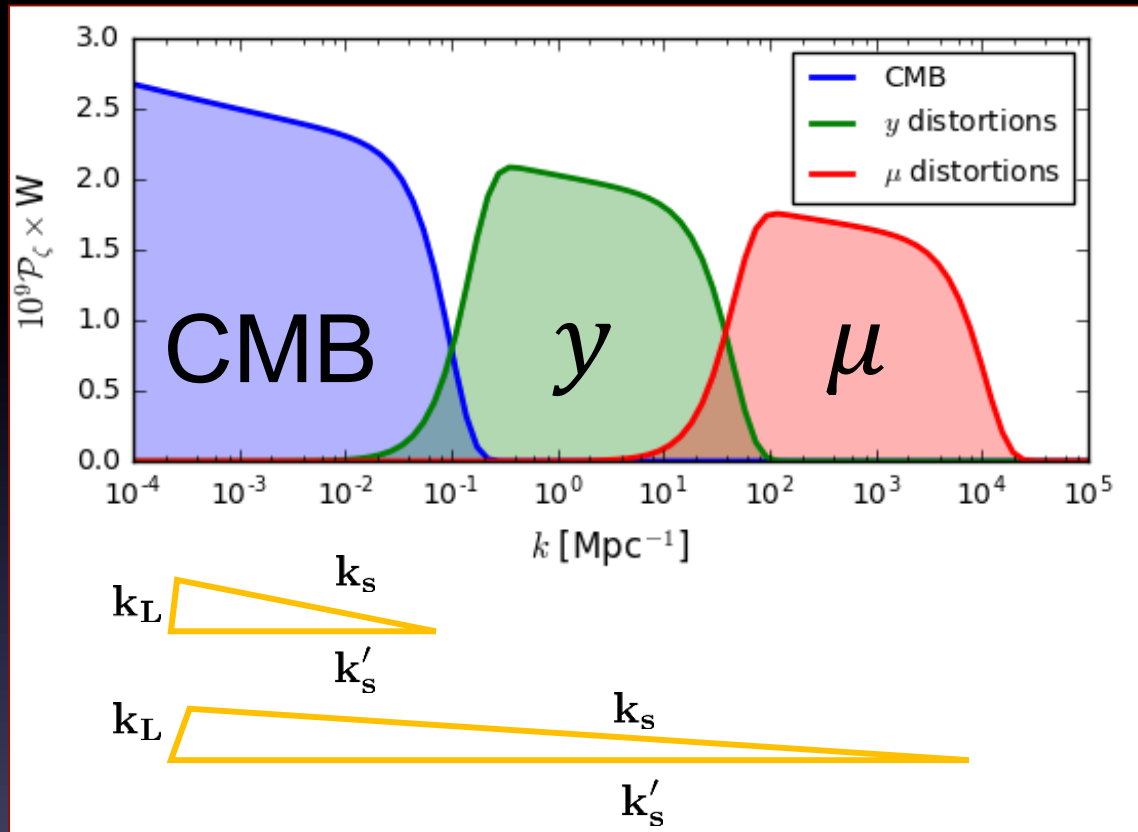








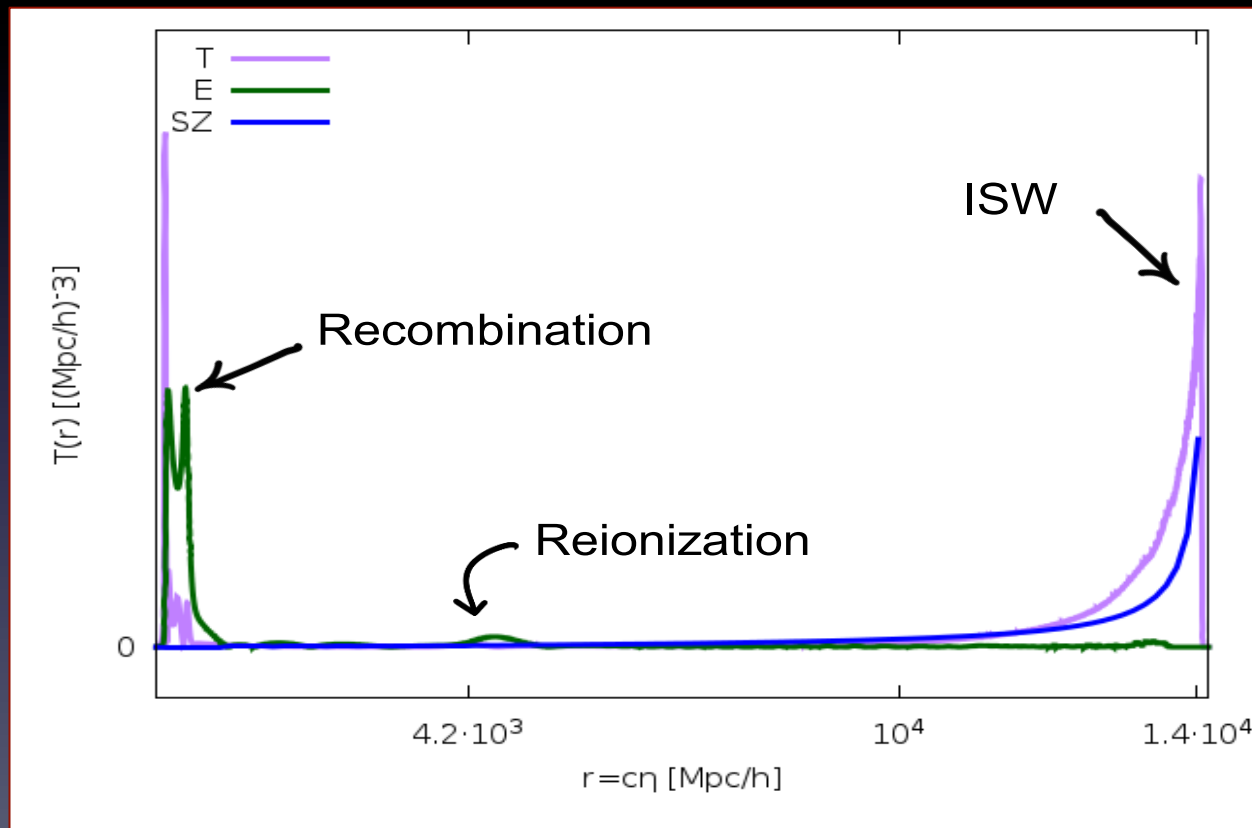
# Testing $f_{NL}$ running with $\mu$ and $y$ distortions



- Can use  $T_\mu$  and  $T_y$  to measure  $f_{NL}$  at different scales and test running.
- Main problem: SZ effect generates large  $T_y$  (bias) and  $y_y$  (noise) (Emami et al. 2015, Dimastrogiovanni & Emami 2016, Creque-Sarbinowski, Bird, Kamionkowski 2016)

# Remove bias: $\gamma E$ correlation

- SZ-CMB temperature correlation is due to late ISW.
- $\gamma E$  does not contain this spurious, non-primordial signal.



# Mitigate yy noise from SZ

- Mask resolved clusters, exploiting external datasets (e.g e-Rosita)
- For diffuse y component from unresolved cluster: exploit cross-correlation with external tracers (lensing) to build a SZ y-map template, and subtract
  - Use halo model to calculate SZ power spectrum
  - Use halo model to calculate Lensing-SZ cross-correlation
  - Consider ML estimator of SZ y-map, given observed lensing map

$$p(a_{\ell m}^{\text{SZ}} | \mathbf{t}_{\ell m}) = \mathcal{N}(\mathbf{C}_{\ell}^T \mathbf{B}_{\ell}^{-1} \mathbf{d}_{\ell m}, \mathbf{C}_{\ell}^{\text{SZSZ}} - \mathbf{C}_{\ell}^T \mathbf{B}_{\ell}^{-1} \mathbf{C}_{\ell}) \Rightarrow \hat{a}_{\ell m}^{\text{SZ}} = \mathbf{C}_{\ell}^T \mathbf{B}_{\ell}^{-1} \mathbf{d}_{\ell m}$$

➤ Subtract

$$a_{\ell m}^{\text{clean}} = a_{\ell m}^{\text{obs}} - \hat{a}_{\ell m}^{\text{SZ}} \quad p(a_{\ell m}^{\text{clean}} | \mathbf{t}_{\ell m}) = \mathcal{N}(-\mathbf{C}_{\ell}^T \mathbf{B}_{\ell}^{-1} \mathbf{t}_{\ell m}, \text{Var}(a_{\ell m}^{\text{obs}}) + \text{Var}(\hat{a}_{\ell m}^{\text{SZ}}) - 2\text{Cov}(a_{\ell m}^{\text{obs}}, \hat{a}_{\ell m}^{\text{SZ}}))$$

# Non-linear kinetic SZ

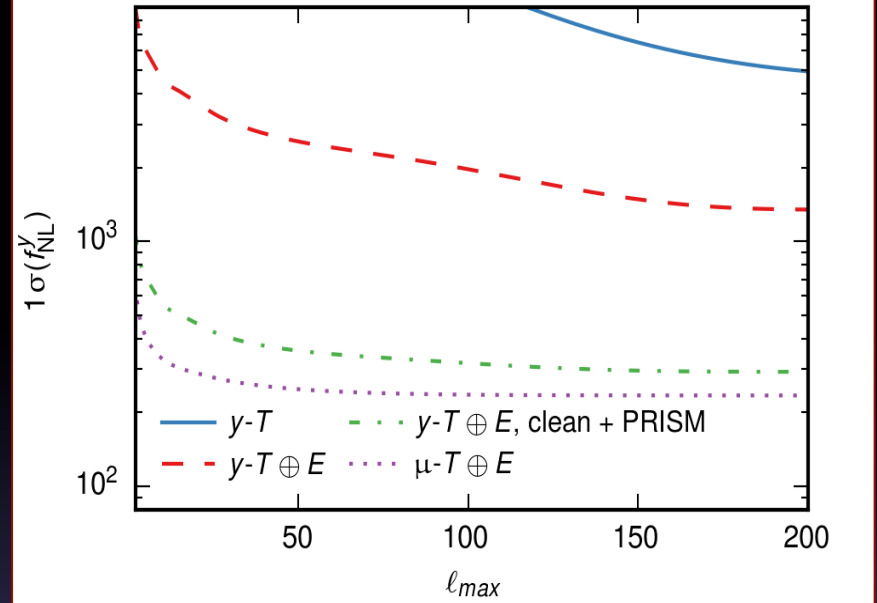
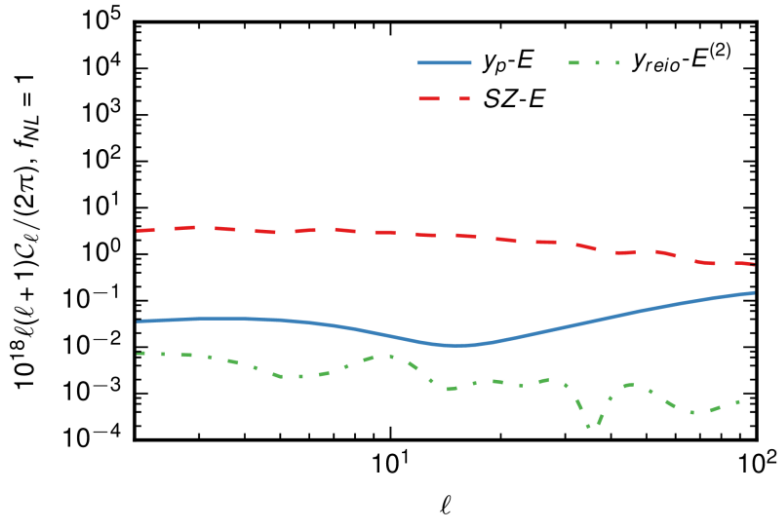
- After reionization, free electrons source  $\gamma$ -distortions. Non-linear kinetic SZ due to bulk motion of free electrons. Proportional to  $v_b^2$
- Correlation with polarization sourced at reionization  $y_{\text{reio}} E = y_{\text{reio}} E^{(1)} + y_{\text{reio}} E^{(2)} + \dots$
- Leading order  $\sim$  trispectrum

$$\begin{aligned}
 y_{\text{reio}}^{(2)} - E^{(2)} = & (-1)^{\ell' - m} 64\pi \int \frac{q_1^2 dq_1 q_2^2 dq_2}{(2\pi)^3} \int \frac{k_1^2 dk_1}{(2\pi)^3} P(q_1) P(q_2) \delta_{\ell}^{\ell'} \delta_m^{-m'} \\
 & \left[ \overline{\mathcal{T}}_{X \ell, 0}^{(2)}(q_1, q_2, k_1) \frac{1}{3} I_{\ell'}^{(1)}(q_1, q_2, k_1) \int x^2 dx j_0(xk_1) j_1(xq_1) j_1(xq_2) + \right. \\
 & + \sum_L \sum_{L_1} \sum_{m_1} \sum_{n=-1}^1 \overline{\mathcal{T}}_{X \ell m_1}^{(2)}(q_1, q_2, k_1) \frac{11\pi}{45} I_{\ell', m_1}^{(2)}(q_1, q_2, k_1) (-1)^{L_1+1} i^{L+L_1+1} (-1)^{3m_1} \\
 & \begin{pmatrix} L_1 & 1 & L \\ 0 & 0 & 0 \end{pmatrix} \begin{pmatrix} L_1 & 1 & L \\ n & -n & 0 \end{pmatrix} \begin{pmatrix} L_1 & |m_1| & 1 \\ 0 & 0 & 0 \end{pmatrix} \begin{pmatrix} L_1 & |m_1| & 1 \\ -n & m_1 & -m_1 + n \end{pmatrix} \\
 & \left. \frac{3(2L+1)(2L_1+1)}{4\pi} \alpha_{n, m_1} \int x^2 dx j_L(xk_1) j_{L_1}(xq_1) j_1(xq_2) \right].
 \end{aligned}$$

- We computed the correlation numerically. 2<sup>nd</sup> order E transfer functions computed with SONG (Pettinari et al. 2014)

# Forecasts

yE



## PIXIE

	Mask	$T$	$T \oplus E$	$T \oplus E$ , clean.
$1\sigma(f_{\text{NL}}^y)$	Unmasked	12700	3300	2900
	eROSITA	8600	2700	2300

## PRISM

	Mask	$T$	$T \oplus E$	$T \oplus E$ , clean.
$1\sigma(f_{\text{NL}}^y)$	Unmasked	4900	1700	1300
	PRISM	1000	380	300

## Cosmic Variance Limited

	Mask	$T$	$T \oplus E$	$T \oplus E$ , clean.
$1\sigma(f_{\text{NL}}^y)$	Unmasked	2300	1000	750
	PRISM	400	160	130

Overall factor  $\sim 16$  improvement (PRISM)  
From masking + template cleaning + yE

20% improvement on  $\mu T$  when  
adding  $\mu E$  (see also Ota 2016)

# Conclusions

- The  $\mu\mu T$  bispectrum carries interesting extra information about PNG, with respect to  $\mu\mu$ ,  $\mu T$ . It allows building (unbiased)  $g_{NL}$  estimators.
- As usual, since one integrates over lots of modes up to very high  $k$ , the potential of an ideal survey is impressive:  $g_{NL} < 1$
- In practice, requires  $\sim 1000$  smaller noise power than a CMBpol-like survey to improve over current Planck bounds (very optimistic, neglects foregrounds and systematics)
- Correlating spectral distortions with polarization is also interesting. Besides obvious error bars improvements,  $\gamma E$  does not display SZ contamination. Useful especially for  $f_{NL}$  running
- Combining  $\gamma T + \gamma E$  with cluster masking and  $\gamma$ -map template removing we achieve a factor  $\sim 16$  improvement on  $\gamma$ -based  $f_{NL}$  forecasts